Networking of optical fiber sensors for extreme environments

Kara Peters

Department of Mechanical and Aerospace Engineering, North Carolina State University, Campus Box 7910, Raleigh, NC, 27695 USA

ABSTRACT

One of the major benefits of optical fiber sensors for applications to structural health monitoring and other structural measurements is their inherent multiplexing capabilities, meaning that a large number of sensing locations can be achieved with a single optical fiber. It has been well demonstrated that point wise sensors can be multiplexed to form sensor networks or optical fibers integrated with distributed sensing techniques. The spacing between sensing locations can also be tuned to match different length scales of interest. This article presents an overview of directions to adapt optical fiber sensor networking techniques into new applications where limitations such as available power or requirements for high data acquisition speeds are a driving factor. In particular, the trade-off between high fidelity sensor information vs. rapid signal processing or data acquisition is discussed.

Keywords: Fiber Bragg gratings, multiplexing, sensor networks

1. INTRODUCTION

Researchers have demonstrated for decades that a major benefit of optical fiber sensors, and in particular fiber Bragg grating (FBG) sensors is their multiplexing capabilities.[1] The term multiplexing refers to collecting a large number of sensors within a single measurement channel (in this case an optical fiber), with the ability to collect both the signal output from each sensor in the channel, but also identify from which sensor each signal output originated. In comparison to many electrical based sensor systems, in which a separate lead-in and lead-out connection is required for each individual sensor, multiplexing allows many sensors to be interrogated quickly with only a single connection to all sensors. The reduction in lead wires typically results in a reduction of the hardware complexity of sensor networks, as well as a reduced perturbation to the material system if the sensor network is to be directly embedded in the material. For large, weight-critical structural applications the weight reduction in lead wires enabled by multiplexing can be a major advantage.[2] A particular multiplexing scheme is defined not only by the arrangement of sensors within the optical fiber, but also the interrogation method used to collect data from the sensors and is therefore a combined hardware and software system.

When designing a multiplexed sensor network, there are a number of tradeoffs, at least some of which must be considered for a given application. Examples of these tradeoffs include the:

- number of sensors
- total data acquisition time
- data acquisition rate
- light source bandwidth
- wavelength resolution
- data processing speed
- sensor fidelity information

Some of these tradeoffs, such as sensor fidelity information cannot be obtained strictly from the FBG peak wavelength information. The goal of this paper is to show how the range of some of these tradeoffs can be expanded using FBG sensor metadata. Therefore, one would add the *amount of sensor metadata to be captured* to the tradeoff list above. Section 2 explains what is meant by FBG sensor metadata in this context and how it would be used in sensor network applications. This article also shows applications of the use of sensor metadata

Send correspondence to K.P. E-mail: kjpeters@ncsu.edu, Telephone: 1 919 515 5226

Sensors and Smart Structures Technologies for Civil, Mechanical, and Aerospace Systems 2016, edited by Jerome P. Lynch, Proc. of SPIE Vol. 9803, 980303 · © 2016 SPIE
CCC code: 0277-786X/16/$18 · doi: 10.1117/12.2225296

in sensor networks expands sensor capabilities in extreme environments. For the sake of discussion, extreme environments are environments which push the envelope of sensor network capabilities, rather than the limits of the sensors themselves. Some examples would include sensor applications for the measurement of:

- dynamic events for which high data acquisition rates are required;
- applications for which spectral distortion due to high temperature or strain gradients or even sensor failures are expected;
- applications for which the available power for interrogation of the sensor network is limited;
- highly dense sensor networks for which a large number of sensors must be interrogated.

2. BACKGROUND

FBGs are wavelength filters created by a periodic modulation in the index of refraction of an optical fiber core. A narrowband spectrum is reflected back from the FBG when a broadband of light is input into the optical fiber, determined by the amplitude and period of the index modulation, as shown in figure 1. When temperature changes or strain components are applied to the FBG sensor, the reflected spectrum shifts to high or lower wavelengths. The peak shift of the reflected spectrum, $\Delta\lambda_B$, is therefore directly related to the applied strain or temperature through,

$$\Delta\lambda_B = s_\epsilon \epsilon + s_T \Delta T \tag{1}$$

where ϵ and ΔT are the applied axial strain and temperature, and s_ϵ and s_T are the sensitivities of the FBG to strain and temperature. Both s_ϵ and s_T are functions of the index modulation properties, the optical fiber material and optical properties. As the index modulation is along a local length, an individual FBG is sensitive to strain and temperature changes only at that location. Since the strain or temperature information is encoded in the shift of the peak wavelength, common FBG measurement devices measure this peak spectrum shift. A list of these interrogation methods will not be included here, but a common example is to pass the reflected spectrum of the FBG through a separate wavelength filter. The output of the wavelength filter can then be calibrated as a function of peak wavelength location.[1] More sophisticated methods also exist for better determining the peak wavelength location in the presence of measurement noise. What is important for this discussion is that FBG peak wavelength measurements can be made at high data acquisition speeds and at high accuracy for FBG sensor networks.

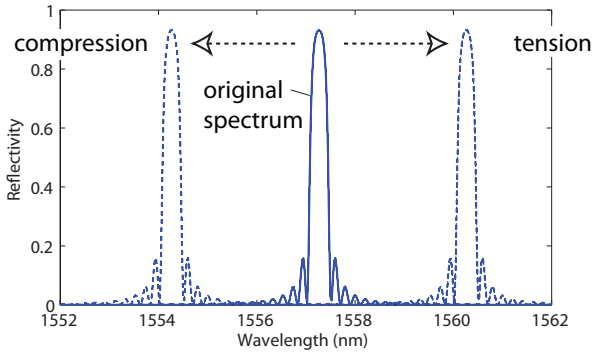

Figure 1. Schematic of FBG sensor reflected spectrum under various strain states.

Classical multiplexing techniques for FBG sensor networks include (i) wavelength division multiplexing in which the wavelength range of the input laser is divided into individual windows for each sensor; (ii) time division multiplexing (TDM) in which the same wavelength window is used for each sensor, but the sensors are spaced along an optical fiber, such that their reflected spectra arrive at discrete times; and (iii) a combination of wavelength and time division multiplexing which uses both individual sensor windows and time delays to increase

the number of sensors.[1] WDM generally requires a high bandwidth input laser to multiplex a large number of sensors within a single channel. TDM does not require a high bandwidth input laser, but does require large distances between sensors and complex time synchronization of the signals.

In this article, sensor "metadata" will refer to all information contained in the reflected spectrum of a FBG, other than the peak wavelength (or centroidal wavelength). This can be discrete metadata, such as the full width at half maximum or the maximum reflectivity, or the complete spectrum itself. More advanced sensor identification methods have been developed using the spectral metadata, such as spectral division multiplexing where a high frequency modulation is added to the reflected spectrum during fabrication of the FBG.[3] The measurement of peak wavelength shifts are then measured in the standard fashion, however each FBG sensor has a distinct high frequency modulation. Performing an FFT on the wavelength spectrum can produce the location of each individual sensor in the reflected spectrum and therefore its individual wavelength shift. Adding the unique tag to each sensor also has the added benefit that a separate window is not required for each sensor, meaning that multiple sensors can occupy the same window as their central location can be reconstructed from the FFT. However, the disadvantage to this technique is that the superposition of the high frequency modulation during fabrication is complex and limited in the number of sensors due to the discrete frequencies that must be both fabricated and separated using the FFT. However, combining this technique with WDM can certainly increase the number of sensors that can be used in a fixed laser bandwidth.

The following sections present examples of FBG sensor metadata and show three examples of their application. In the first example, the use of metadata eliminates noise due to spectral distortion in FBG dynamic data, preventing misinterpretation of the data. In the second example, metadata is applied to extract transverse loading information from a sensor, while collecting data on other loading directions. In the third example, the interplay between the number of sensors, wavelength resolution and data acquisition speed when collecting FBG data during impact of a composite structure. These examples are meant to be representative, not to show the full range of what can be achieved.

3. EXAMPLE 1

This example demonstrates typical measurement results collected from a FBG sensor embedded in a lap joint, during a structural health monitoring (SHM) scenario.[4] The FBG sensor is embedded in the adhesive layer of a lap joint, subjected to tensile-compressive fatigue loading. The fatigue loading was stopped after discrete numbers of fatigue cycles and the lap joint subjected to a vibration load, in this case 150 Hz, to mimic in-flight airframe loading. By measuring the dynamic response of the FBG sensor to the vibration loading, the extent of damage within the lap joint was to be extracted. Although this example only incorporates a single FBG sensor, the concept would apply to multiplexed sensors as well.

The induced fatigue damage in the joint created a strain gradient along the FBG sensor during the loading of the lap joint, producing spectral distortion. This distortion can be seen in figure 2(d), in which the FBG reflected spectrum, measured after fatigue damage was present, is plotted both for the unloaded lap joint and with tension applied to the joint. Prior to fatigue loading, the FBG reflected spectrum was a single peak, similar to that of figure 1. However, due to uneven loading of the FBG, the spectrum is distorted into two peaks. With the application of tensile loading to the joint, the strain gradient and therefore the distortion are increased, pushing the two primary peaks apart and reducing the reflectivity of the FBG.

The FBG peak wavelength measurements were collected to determine the dynamic response of the joint during vibration loading, and therefore evaluate the remaining fatigue life of the joint. The measurement results after 1000 cycles of fatigue loading are shown in figure 2. Figure 2(a) shows the raw full-spectral data collected over 30 ms. Full-spectral measurements of the FBG response were collected during the vibration loading, such that the measured peak wavelength response could be calculated and the effects of potential distortion evaluated. From this data, the peak wavelength location was calculated as a function of time and the short time Fourier transform (figure 2(b)) and its corresponding phase-plane diagram (figure 2(c)) calculated from this peak location. In figures 2(b) and (c) the peak wavelength data was extracted by choosing the wavelength at maximum intensity. In figure 2(c) the phase state is localized at four different locations within the phase plane, with wavelength shifts up to 1.0 nm, typical of a system with a quasi-period response, indicating imminent failure of the joint.

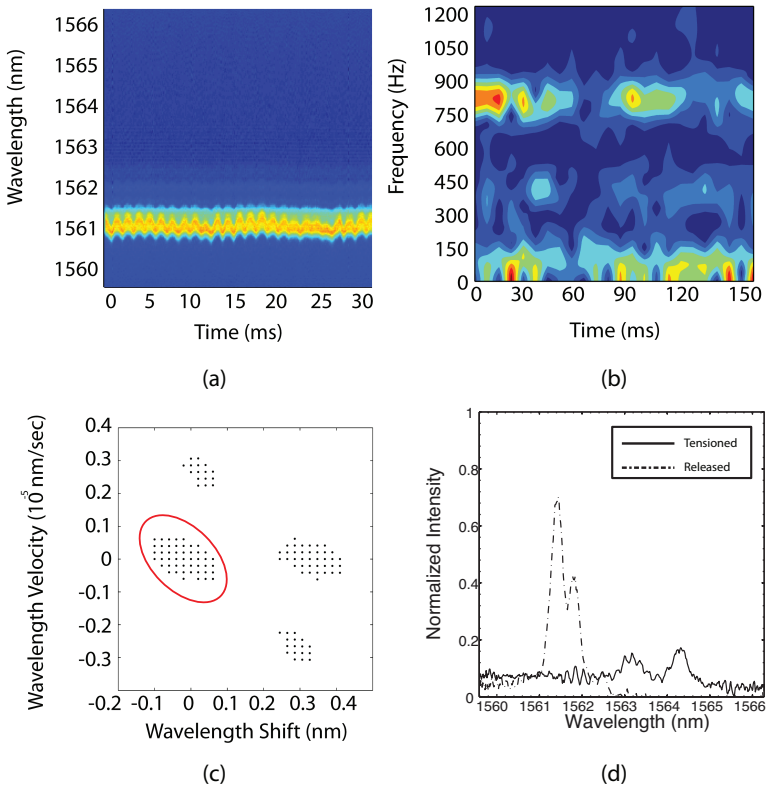

Figure 2. (a) Raw full-spectral data after 1000 cycles of fatigue loading. Color scale is reflected intensity with red the highest intensity. (b) STFT computed for entire data set (without wavelength hopping correction). (c) Phase-plane diagram calculated from FBG spectra data set without peak location correction. Red oval shows the only set of points calculated when the peak location correction is applied. (d) Measured full-spectral FBG response immediately after 1000 cycles of fatigue during pretensioning and release.[4]

In a second analysis, the peak wavelength data was also extracted for the same loading case from the data of figure 2(a) following the primary peak, identified based on the full-spectrum metadata, even if its maximum intensity went below the other peak. For this case, the phase state was localized within the single, narrow region of the phase plane shown as the red oval in figure 2(c), typical of a system with a linear response. This second interpretation was confirmed to be correct through infrared imaging of the adhesive layer in the lap joint.[4] The difference in the phase plane representations is due to the multiple-peak FBG reflected spectrum with near-equal intensities, as seen in figure 2(d). As the spectral distortion was high the wavelength at maximum intensity randomly varied between the the two peaks, with an approximately 1 nm spacing, resulting in the phase-plane diagram data jumping between the four regions in figure 2(c).

4. EXAMPLE 2

The second example considers another use of distortion to the FBG spectra, again only captured if the full spectrum metadata is collected, to provide additional information about the state of the FBG and therefore the state of the material surrounding the FBG. Another potential source of distortion to a FBG reflected spectrum is through a superimposed period index modulation along the FBG, for example due to applied stress, on top of the original index modulation of the FBG. In the case where the superimposed modulation is of a significantly higher period, this is referred to as *superstructuring* of the FBG. Superstructuring can only be measured when a large range of the reflected spectrum is captured. This measurement requires a wider wavelength sweep than the other spectrum metatdata. One example of the use of superstructuring metadata is shown in Figure 3 in which a FBG was embedded in a 2x2 twill woven composite.[5] After multiple impacts to the laminate composite, residual stresses built up through the thickness of the composite, resulting in a through-the-thickness compressive stress

on the embedded FBG. A measured reflected spectrum from the FBG is shown in figure 3, both before and after a significant impact event.

In this example, the reflected spectrum is not a smooth curve, both before and after the impact event. There appears to be a rough wavelength modulation on the expected spectrum. This modulation was increased after the impact event and was assumed to be due to the transverse pressure on the FBG due to the 2x2 woven geometry of the material layers above and below the FBG. In order to confirm that these multiple peaks were in fact due to superstructuring, the theoretical peak spacing was calculated for this example using

$$\Delta\lambda = \frac{\lambda_B^2}{2n_{\text{eff}}\Lambda_e} \tag{2}$$

where Λ_e is the envelope period due to the periodic pressure, λ_B is the Bragg wavelength of the FBG and n_{eff} is the effective fundamental mode index of the optical fiber.[6] For this example, $\lambda_B = 1564$ nm, $n_{\text{eff}} = 1.47$ and Λ_e is the known 2 mm weave spacing of the two-dimensional twill material, yielding $\Delta\lambda = 0.41$ nm. This wavelength spacing is superimposed on the curves of figure 3 and approximates the measured peak spacing.

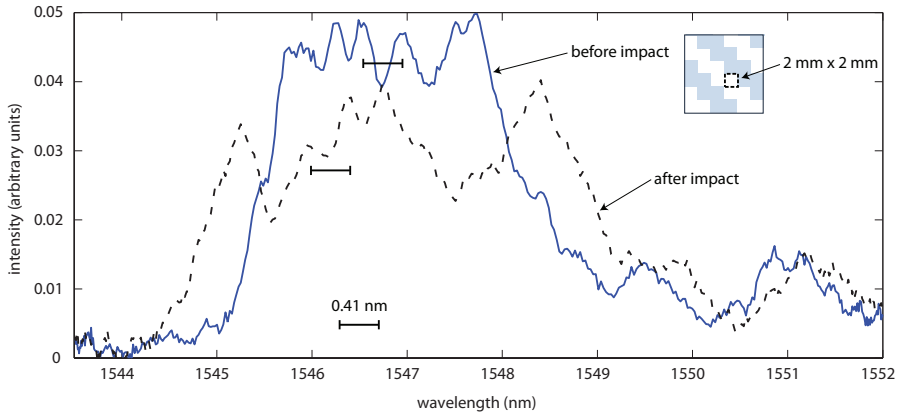

Figure 3. Wavelength sweeps measured before and after impact for strike 110 of Specimen 1. Inset shows 2x2 twill geometry of woven carbon fiber.[5]

5. EXAMPLE 3

The last example considers a measurement case with multiplexed sensors, in which the network settings are dependent upon several of the tradeoffs listed in section 1. In this example, a high-speed, full-spectral interrogator was applied to measure the impact response of a series of multiplexed FBG sensors embedded in a stiffened composite structure.[7] The structure was subjected to a low-velocity impact by hitting it with an impact hammer.

The full spectral interrogator was based on a narrowband MEMS tunable filter, driven with a sinusoidal driving voltage. For high-speed measurements of dynamic events, the limiting factor is generally the total amount of measurement points that can be collected and saved in a short amount of time, generally on the order of GBs. The number of data points depends on the data acquisition frequency and the total measurement time. In addition, the driving frequency of the tunable filter, combined with the data acquisition rate determines the wavelength and temporal resolution of the measurement. The overall system envelope for a fixed maximum number of data points M can be written as

$$\frac{WT}{\Delta\lambda\Delta t} \leq 0.4M \tag{3}$$

where W is the wavelength range of the tunable filter, T is the measurement duration, $\Delta\lambda$ is the wavelength resolution and Δt is the temporal resolution.[7] The factor of 0.4 comes from the fraction of the sinusoidal curve

that is used for the rising and falling measurement sweeps. It is also important to note that for mechanical filters, the wavelength range W is a nonlinear function of the driving frequency.

The response of several multiplexed sensors are shown in figures 4(a) and (b), varying the data acquisition parameters. The impact event is clearly visible in both measurements. The number of FBG sensors visible was maximized in the measurement of figure 4(a) using a resolution of 0.1 ms, however several discontinuities are visible in this measurement where the peak information of some sensors was lost, for example at $t = 371$ ms. The measurement was then repeated, reducing the number of sensors that could be monitored, but with an increased temporal resolution of 0.01 ms, shown in figure 4(b). The number of sensors was reduced due to the increased filter driving frequency and therefore decreased filter vibration amplitude (or wavelength range). However, due to the increase temporal resolution, more detail is provided on the spectral deformation during the impact event. Figure 4(c) shows a detailed view of one of the FBG sensors from this measurement. In this view, distortion of the spectrum due to the non-uniformity along the FBG as the stress waves passes the FBG can clearly be seen. This distortion provides details on the form of the stress wave as it passes through the material (that cannot be obtained from peak wavelength information), however it is released once the impact event is finished and must therefore be captured at high speeds.

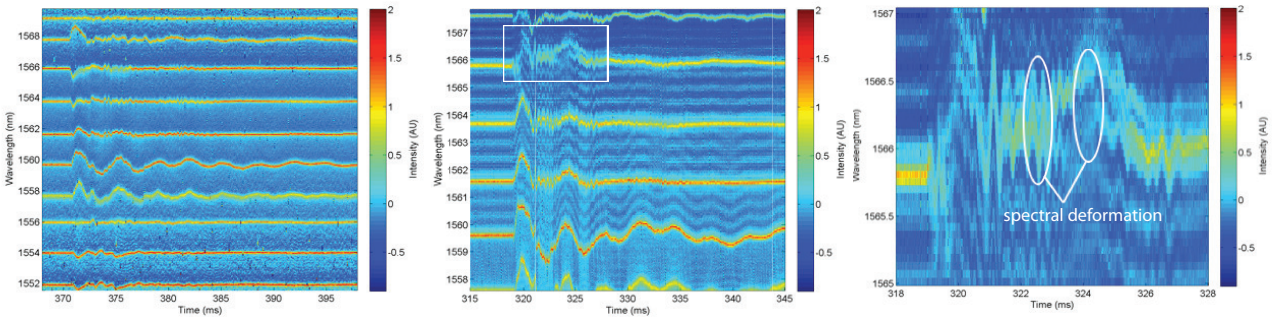

Figure 4. Full-spectral reconstruction of (a) 10 FBG sensors during impact using $\Delta\lambda = 4$ pm at 10 kHz. (b) 6 FBG sensors during impact using $\Delta\lambda = 21$ pm at 10 kHz. (c) Detailed view of 1 FBG sensor from measurements in (b).

6. CONCLUSIONS

This article presented three examples of FBG sensor network metadata that could provide additional information for structural health monitoring applications. In the first two cases, the metadata prevented misinterpretation of data (and could similarly be applied to increase the fidelity of sensor information) or was applied to extract additional information from the sensor. In the final case, the choice of sensor metadata and the resolution with which it was obtained helped to define the sensor network parameters to be used in the measurements.

ACKNOWLEDGMENTS

Research described in this paper has been partially funded by the National Science Foundation through grant CMMI 0900369 and through funds while working at the Foundation. Additionally, the research was partially funded by the ANST Graduate Fellowship Program. Work in this paper has also been partially developed as a result of a mobility stay funded by the Erasmus Mundus Programme of the European Commission under the Transatlantic Partnership for Excellence in Engineering - TEE Project. Thanks are due to Spencer Chadderdon, Bram Van Hoe, Steven Schultz, Nikola Stan, William Stewart, and Sean Webb, for their contributions to the results presented in this paper.

REFERENCES

[1] E. Udd and W. B. Spillman Jr. *Fiber Optic Sensors: An Introduction for Engineers and Scientists*, Wiley, 2011.

[2] B. A. Childers, M. E. Froggatt, S. G. Allison, T. C Moore, D. A. Hare, C. F. Batten and D. C. Jegley "Use of 3000 Bragg grating strain sensors distributed on four 8 m optical fibers during static load tests of a composite structure," in *Smart Structure and Materials 2001: Industrial and Commercial Applications of Smart Structures Technologies*, SPIE **4332**, 2001.

[3] A. C. L. Wong, P. A. Childs and G. D. Peng "Multiplexing technique using amplitude-modulated chirped fiber Bragg gratings," *Optics Letters*, **32**, 1887-1889, 2007.

[4] S. Webb, K. Peters, M. Zirky, S. Chadderdon, N. Stan, R. Selfridge, and S. Schultz "Characterization of fatigue damage in adhesively bonded lap joints through dynamic, full-spectral interrogation of fiber Bragg grating sensors: Part 1. Experiments, *Smart Materials and Structures*, **23**, 025016, 2014.

[5] S. Webb, K. Peters, M. Zikry, T. Vella, S. Chadderdon, S. Schultz, and R. Selfridge "Wavelength Hopping due to Spectral Distortion in Dynamic Fiber Bragg Grating Sensor Measurements, *Measurement Science and Technology*, **22**, 065301, 2011.

[6] B. J. Eggleton, P. A. Krug, L. Poladian and F. Ouellette "Long periodic superstructure Bragg gratings in optical fibres" *Electronics Letters*, **30**, 1620-1622, 1994.

[7] B. van Hoe, K. Oman, K. Peters, G. van Steenberge, N. Stan and S. Schultz "High-speed interrogation of multiplexed fiber Bragg gratings enabling real-time visualization of dynamic events such as impact loading," in *IEEE Sensors Conference*, 2014.